

REINVESTIGATION OF RESONANCE RAMAN SPECTRUM OF
RUTHENIUM RED AND ITS PHOTODEGRADATION

Masao ITABASHI, Kazuo SHOJI, and Koichi ITOH*
Department of Chemistry, School of Science and Engineering,
Waseda University, Shinjuku-ku, Tokyo 160

A photodegradation of Ru-red was found during the analysis of its resonance Raman spectrum; an apparent rate constant of the decomposition has been estimated to be about 10 s^{-1} . Reasonable assignments are given to the Raman bands of Ru-red and its derivatives. A structural model is proposed to the compound in its aqueous solution.

The resonance Raman spectra of ruthenium red and its derivatives have extensively been analyzed by several authors^{1,2)} in view of the importance of the compound ($[(\text{NH}_3)_5\text{Ru}-\text{O}-\text{Ru}(\text{NH}_3)_4-\text{O}-\text{Ru}(\text{NH}_3)_5]^{6+}$, abbreviated to Ru-red) as a cytological reagent,³⁾ as an inhibitor of the active Ca^{2+} -transport,⁴⁾ and especially as a resonance Raman probe¹⁾ for the study of the Ca^{2+} -transport mechanism. Recently we found that Ru-red is very photolabile and the samples used by the former authors^{1,2)} were seriously contaminated with a photodegradation product. In this paper we give more reliable assignments to the observed Raman bands and propose a structural model to Ru-red in its aqueous solution.

Ru-red, Ru-red- d_{42} , ruthenium brown ($[(\text{NH}_3)_5\text{Ru}-\text{O}-\text{Ru}(\text{NH}_3)_4-\text{O}-\text{Ru}(\text{NH}_3)_5]^{7+}$), and an ethylenediamine analog of Ru-red ($[(\text{NH}_3)_5\text{Ru}-\text{O}-\text{Ru}(\text{NH}_2\text{CH}_2\text{CH}_2\text{NH}_2)_2-\text{O}-\text{Ru}(\text{NH}_3)_5]^{6+}$, abbreviated to Ru-red(en)) were synthesized and purified by the procedures⁵⁾ reported previously. The spectra were recorded with a Spex 1401 doublemonochromator. To avoid the decomposition due to laser excitation a flow technique was used, making the flow fast enough ($\text{ca. } 11 \text{ cm s}^{-1}$) so that the decomposition was almost negligible.

Figures 1(A), (C), and (D) give the Raman spectra of Ru-red, Ru-red(en), and Ru-brown, respectively. The spectrum of Ru-red (Fig. 1(A)) is quite different from those already reported^{1,2)} especially in the 850-750 and 500-350 cm^{-1} regions. When the sample flow is stopped, Ru-red gives the spectrum shown in Fig. 1(B). The bands at 414, 451, and 837 cm^{-1} in Fig. 1(B) are due to one of the photodegradation

products. From this result the prominent peaks observed near 410 cm^{-1} by the former authors^{1,2)} can be attributed to the contamination by the photodegradation product. The spectral difference in the $850\text{--}750\text{ cm}^{-1}$ region can also be explained by this contamination. On oxidation of Ru-red to Ru-brown (Fig. 1(D)), the 825-- , 744-- , 281-- , and 157--cm^{-1} bands in Fig. 1(A) shift to higher frequency sides by 15 , 34 , 13 , and 21 cm^{-1} , respectively. The corresponding shifts observed by Campbell *et al.*²⁾ are only 2 , 19 , 7 , and 7 cm^{-1} . Presumably the smaller frequency shifts are due to the incomplete oxidation of Ru-red.

Ru-red and Ru-red(en) in the crystalline state take a nearly linear backbone structure with the μ -oxo and ammine ligands taking an octahedral coordination about the metal atoms. The symmetry of the skeleton of Ru-red, however, is quite different from that of Ru-red(en), the former being close to C_{4v} ⁶⁾ and the latter to D_{4h} .⁷⁾ From their spectra Campbell *et al.* concluded that Ru-red in the solution retains a structure almost identical with the one taken by the solid sample. The spectrum of Ru-red(en) in the solution (Fig. 1(C)), however, is almost identical with that of Ru-red (Fig. 1(A)), indicating that the skeletal backbones of both samples are similar to each other. Therefore, it is more relevant to consider that the backbone of Ru-red in the solution has a symmetry close to D_{4h} .

We measured the excitation profile of the Raman bands of Ru-red in the main ab-

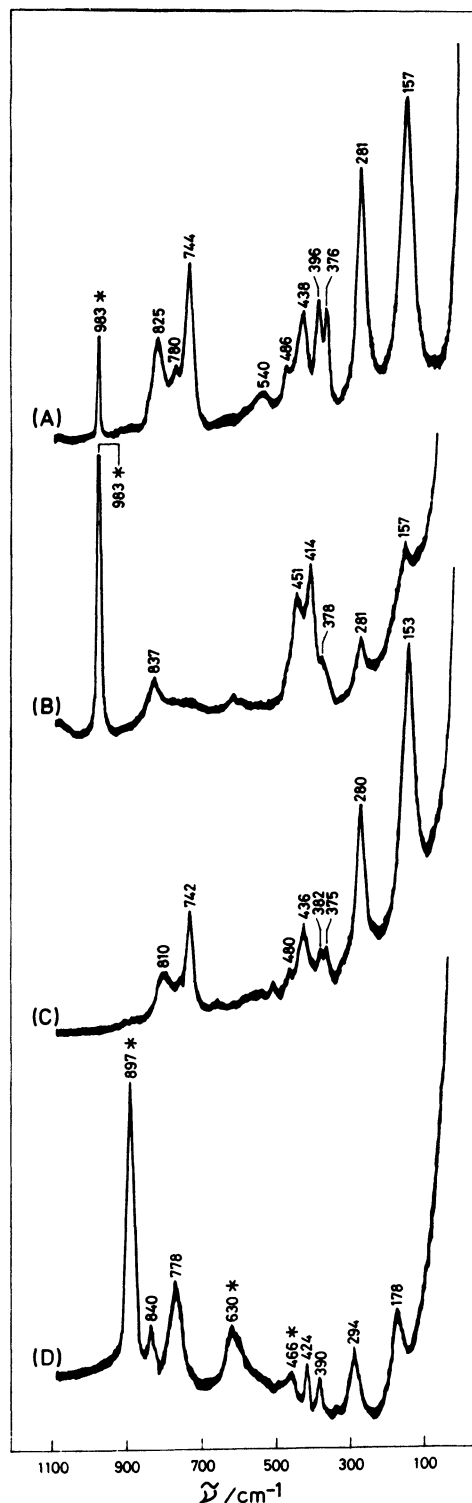


Fig. 1. Resonance Raman spectra of (A) Ru-red in $\text{NH}_4\text{Cl-NH}_3$ buffers (pH 10) before decomposition, (B) Ru-red in $\text{NH}_4\text{Cl-NH}_3$ buffers (pH 10) after decomposition, (C) Ru-red(en) in NH_4Cl aq. soln., and (D) Ru-brown in NaAc-HAc buffers (pH 4). All the spectra were measured at a room temperature by a flow technique except for (B) (see text). Conc., ca. 10^{-4} M . Excitation wavelength, 530.9 nm (Kr^+ laser) for (A), (B), and (C); 476.2 nm (Kr^+ laser) for (D). The starred bands are due to SO_4^{2-} or CH_3COO^- .

sorption region ($\lambda_{\text{max}}=532 \text{ nm}$, $\epsilon=69.9 \times 10^3$). The result, which is similar to that observed by Campbell *et al.*, clearly indicates that the intensities of the 744-, 281-, and 157- cm^{-1} bands in Fig. 1(A) are enhanced in the main absorption region to much larger extents than the 825-, 438-, 396-, and 376- cm^{-1} bands.

On the basis of the experiments mentioned above we reexamined the assignments of the Raman bands of Ru-red and Ru-brown, which are summarized in Table 1 together with the observed frequencies of Ru-red- d_{42} . The vibrational modes are expressed by the notations proposed by Campbell *et al.*. We assigned the 825- and 744- cm^{-1} bands to the $\nu_7(\text{Ru-O})$ and $\nu_1(\text{Ru-O})$ modes, respectively. On the other hand, Campbell *et al.* ascribed the 827- and 742- cm^{-1} bands in their spectra to the ν_1 mode and rocking vibration of the ammine groups, respectively. To the latter mode we assigned a weak band at 780 cm^{-1} in Fig. 1(A). The prominent feature of the 744- cm^{-1} band and its excitation profile support our assignment. The infrared spectrum of Ru-red in the solid state shows the Ru-O asymmetric stretching ($\nu_7(\text{Ru-O})$) mode at 805 cm^{-1} .⁵⁾ We considered the 825- cm^{-1} band in Fig. 1(A) corresponds to the infrared band. The small deuteration shift ($\Delta\nu=-3 \text{ cm}^{-1}$) observed for this band is consistent with this conclusion. The fact that the ungerade-like mode is observed in the Raman spectrum suggests that the backbone structure of Ru-red does not have any inversion symmetry in its strict sense.

According to the molecular orbital scheme proposed by Earley and Fealey,⁵⁾ the oxidation of Ru-red to Ru-brown is accompanied by the removal of an electron from the b_{1u} orbital located mainly on the terminal Ru atoms. The large difference

Table 1. Obsd. Raman Frequencies of Ru-red and Ru-brown.

| Ru-red | Ru-red- d_{42} | Ru-brown | Assignment ^a . |
|---------|------------------|----------|---------------------------------------|
| 157 ss | 146 s,b | 178 m | $\nu_6(\nu(\text{Ru-O}))$ |
| 281 ss | 250 s | 294 m | $\nu_5(\delta(\text{ORuNeq}))$ |
| 376 m | 355 m | 390 w | } $\nu_{2,3,4,8,9}(\nu(\text{Ru-N}))$ |
| 396 m | 385 m | | |
| 438 m | 402 m | 424 w | |
| 486 sh | 430 sh | | |
| 540 w,b | 610 w,b | | |
| 744 s | 704 m | 778 m | $\nu_1(\nu(\text{Ru-O}))$ |
| | 760 w,b | | |
| 780 w,b | | | $r(\text{NH}_3)$ |
| 825 m | 822 m | 840 w | $\nu_7(\nu(\text{Ru-O}))$ |

Abbreviations: s, strong; m, medium; w, weak; b, broad; sh, shoulder; ss, strong and sharp. ν , δ , and r represent stretching, bending, and rocking modes, respectively. a. see text.

in the frequency of Raman bands between Ru-red and Ru-brown, however, clearly shows that the electron is removed from an anti-bonding orbital which is located on the Ru-O-Ru-O-Ru backbone. Therefore we assigned the e_u^* orbital to the highest occupied one and

concluded that Ru-red has a ground-state electronic configuration of $(e_g^o)^4 (e_u^o)^4 (b_{1g})^2 (b_{1u})^2 (b_{2g})^2 (e_g)^4 (e_u^*)^4$.

As mentioned above, Ru-red in an aqueous solution decomposes upon continuous irradiation of a laser light (e.g., the 514.5 nm line of Ar^+ laser), which can be clearly illustrated by Figure 2. As the flow rate is decreased, the relative intensities of the Raman bands from Ru-red decrease (Figs. 2(B) and (C)) while the intensity of the band around 410 cm^{-1} increases. (We used the 983-cm^{-1} band as an internal standard.) On stopping the sample flow, the solution gives the spectrum shown in Fig. 2(D), which is almost identical with that in Fig. 1(B). The latter spectrum was obtained from the solution irradiated by the 530.9 nm Kr^+ laser light for about 1 h. Assuming a first-order process to the decomposition we estimated the apparent rate constant to be about 10 s^{-1} . The dependence of the rate constant on the sample condition (e.g., pH and temperature) will give more detailed informations about the mechanism of this process.

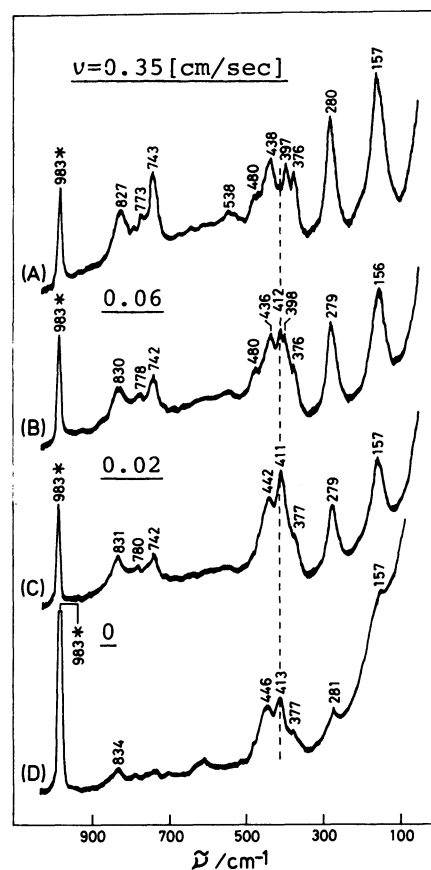


Fig. 2. Dependence of the Raman spectra of Ru-red on the flow rate. ($25^{\circ}C$; ca. 10^{-4} M in NH_4Cl-NH_3 ; 514.5 nm excit. (Ar^+ laser)).

References

- 1) J.M.Friedman, D.L.Rousseau, G.Navon, S.Rosenfeld, P.Glynn, and K.B.Lyons, *Arch. Biochem. Biophys.*, **193**, 14 (1979).
- 2) J.R.Campbell, R.J.H.Clark, W.P.Griffith, and J.P.Hall, *J. Chem. Soc., Dalton Trans.*, **1980**, 2228 (1980).
- 3) J.H.Luft, *Anat. Rec.*, **171**, 347 (1971).
- 4) K.C.Reed and F.L.Bygrave, *Biochem. J.*, **140**, 143 (1974).
- 5) J.E.Earley and T.Fealey, *Inorg. Chem.*, **12**, 323 (1973).
- 6) M.A.A.F.de C.T.Carrondo, W.P.Griffith, J.P.Hall, and A.C.Skapski, *Biochim. Biophys. Acta*, **627**, 332 (1980).
- 7) P.M.Smith, T.Fealey, J.E.Earley, and J.V.Silverton, *Inorg. Chem.*, **10**, 1943 (1971).

(Received February 6, 1981)